

***In-vitro* bacterial adhesion study on stainless steel 316L subjected to magneto rheological abrasive flow finishing.**

Kathiresan S^{1*}, Mohan B²

¹Department of Mechanical Engineering, MNM Jain Engineering College, Chennai, India

²Department of Mechanical Engineering, Anna University, Chennai, India

Abstract

Objective: To study the effect of Magneto rheological abrasive flow finishing (MRAFF) of stainless steel 316L (SS316L) on bacterial adhesion.

Methods: In the MRAFF process, four different SS316L samples were obtained by varying the magnetic flux density from 0.06 tesla to 0.247 tesla by varying the electromagnetic current. In order to study the bacterial adhesion behavior on SS316L samples with respect to the surface roughness at nano level, three different medically significant bacteria such as *Escherichia coli*, *Klebsiella pneumonia* and *Bacillus subtilis* were used and bacterial adhesions were studied by means of Colony Forming Units (CFU) plate counting. In order to visualize the bacterial attachments with the metallic surface, epifluorescent images were used.

Results and discussion: The average surface roughness of the samples was decreasing with the increase of magnetic flux density and they were analysed by means of Coherence Correlation Interferometer (CCI). The range of nano level surface roughness values obtained on the steel surface is 10.52 nm to 37.4 nm. With the same sample surface roughness of 37.4 nm, the bacteria *Klebsiella pneumonia* has got highest adherence of 47×10^8 CFU/ml and *Escherichia coli* has got least adherence of 28×10^8 CFU/ml. The inhibit nature of the 316L stainless steel towards the bacterial attachment was higher for *Escherichia coli* with 19×10^8 CFU/ml for the sample with the minimum average surface roughness, while for the other two bacteria, the inhibition were least and identical with 13×10^8 CFU/ml.

Conclusion: From the experimental results with respect to the bacterial Colony Forming Units (CFU), it was observed that the attitude of bacterial adhesion was more on higher surface roughness and less at the least surface roughness in the period of incubation of 18 h. It also depends on the type of the bacterial cell and its geometry.

Keywords: Magneto rheological, Stainless steel 316L, Bacterial adhesion, Surface finish.

Accepted on December 9, 2016

Introduction

Stainless steel 316L is an ease metallic biomaterial, with a sensible biocompatibility and simple to machine; consequently it is broadly utilized for orthopaedic, cardiovascular and craniofacial applications because of its good corrosion resistance and formability [1]. The surface roughness of the implant material highly influences its biocompatibility. If the surface roughness is reduced from 4.5 micro meters to 200 nano meters, the avenues of cell sustainability were increased by 20 times [2]. This phenomenon is well suited for fibroblast and osteoblast cells towards the improvement of biocompatibility. But, at the same time there is a significant necessity to study the response of bacterial attachment on the implant materials with nano level surface roughness. After implantation, metallic implants by and large turn out to be suddenly typified by a sinewy tissue of up to 200 μ m of thickness, because of a nearby provocative response, that

permits the dispersion of particles and micro particles and impedes the mechanical reliability of the implant. Likewise, a vital issue related to the utilization of implants is the presence of diseases because of the bacterial surface colonization and later development of biofilms, which regularly prompts the failure of medical devices [3-7].

The colonization of bacteria on the medical implant surfaces is a critical medicinal issue, which frequently prompts the failure of therapeutic devices. The attachment of bacteria and the components that impact the procedure, together with the ensuing biofilm arrangement, have been the center of serious study in the course of recent decades [8-11], predominantly because of the progressing push to outline antibacterial surfaces or micro textured surfaces with an effect of antifouling. The components that control bacterial grip have been tended to on different levels: hypothetical methodologies, for example, the Derjaguin, Landau, Verwey, Overbeek and

thermodynamic hypotheses have uncovered a percentage of the essential physicochemical nature of bacterial bond [9,12,13] and studies about cell have given useful information that the cell surface attributes play in the mechanism of bacterial attachment [14,15]. Aside from the cell surface attributes, now a days it is generally acknowledged that an extensive variety of surface properties such as morphology, surface science, surface roughness and porosity would all be able to apply a solid impact over the propensity of bacterial attachment with various surfaces [11,16].

The bacterial attachments on the different surfaces are especially influenced by the qualities of the microorganisms and the type of surface [17]. At the point when microbes approach a surface, they should come out of the energy barrier so as to set up direct contact with the surface. The attractive or repulsive forces comprise of Lifshitz eVander Waals attractive forces, forces due to electrostatic repulsion and acid base forces. As a distorted dependable guideline, essential attachment among microscopic organisms and abiotic surfaces is for the most part interceded by interactions of non-specific nature [18]. Just when the cells and surfaces are in close vicinity, the interaction at short-span becomes noteworthy together with interaction due to hydrophobic nature and hydrogen bonding.

Table 1. Composition of stainless steel 316L.

Element	C	Si	Mn	P	S	Cr	Mo	Ni	Co
Comp (%)	0.03	0.43	1.48	0.03	0.002	16.45	2.11	10.14	0.154
Element	Cu	Nb	Ti	V	W	Fe			
Comp (%)	0.201	0.021	0.012	0.047	0.081	68.812			

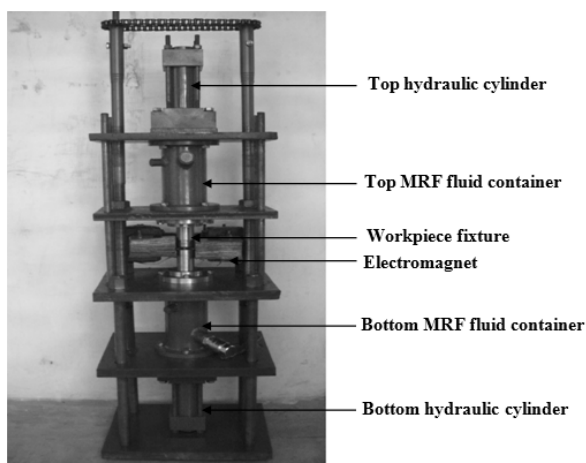


Figure 1. MRAFF experimental setup (Available in the Fluid Power Laboratory, Department of Production Technology, Anna University, Chennai, India).

The constituent of MRA fluid are iron particles, silicon carbide abrasive particles of selective volume percentages with a base fluid of paraffin oil and a suitable surfactant to keep the constituent particles in a Brownian motion.

In light of these current contemplations, the article meant to test whether the surface roughness at nano level assumes a part on the underlying phase of bacterial adhesion. In this experimental work, the impact of nano level surface roughness generated by MRAFF process on stainless steel 316L on the adhesion behaviors of three medically significant bacteria such as *Escherichia coli*, *Bacillus subtilis* and *Klebsiella pneumonia* have been explored.

Materials and Methods

MRAFF nano finishing process

The experimental setup for MRAFF process consists of components as shown in Figure 1. The SS316L work piece of size 40 × 10 × 4 mm on which nano finishing is to be done was kept in the fixture for the work piece. The initial surface roughness of the steel surface was 0.2 μm obtained by plain surface grinding. The composition of SS 316L is given in Table 1. The Magneto Rheological Abrasive (MRA) fluid was filled in the respective fluid containers of the experimental setup.

In the beginning of MRAFF process, the required pressure, current (I) to the electromagnet and number of cycles were set in the programmable logic controller (PLC) program in order to automate the process. The iron particles present in the MRA fluid within the work piece fixture will be in scattered form when there is no magnetic field is generated by the electromagnet. In the presence of current to the electromagnet, the iron particles present in the magneto rheological fluid accumulates like chains [19] and the stiffness of this structure depends on the amount of magnetic flux generated. The ferrous chains along with abrasive particles are reciprocated by means of sequential operation of hydraulic cylinders with sufficient pressure. With respect to the strength of the ferrous chain, abrasive particles captivated by them and hydraulic pressure, expulsive force will be applied and metal removal takes place.

The amount of magnetic flux density generated with respect to the variation of electromagnetic current was calculated by using Equation 1

$$B.G = \mu NI \rightarrow (1)$$

In this equation,

I-Current in Amps ; N - Number of turns in the coil (17 swg copper wire); G-Pole gap in meters (opening of the “C”); B-

Magnetic induction in Tesla (10,000 gauss); μ -Magnetic permeability ($4\pi \times 10^{-7}$)

Four different SS316L samples were obtained by means MRAFF process are given in Table 2 along with the electromagnetic current and the respective magnetic flux density.

Table 2. MRAFF process parameters for SS316L samples.

Parameters	Samples			
	A	B	C	D
Current (Amps)	8A	6A	4A	2A
Magnetic flux density B (Tesla)	0.247	0.185	0.124	0.06

Surface measuring technique

The different surface roughness values generated on SS 316L samples by means of MRAFF processes were examined by talysurf CCI where the measurement area was 6.6 mm square and 0.8 mm of cut-off length was followed. The roughness parameters as well as three dimensional surface images were obtained by the interferometer.

Bacterial adhesion tests

Preparation of nutrient broth: Peptone of 0.3 g, yeast extract of 0.18 g, sodium chloride of 0.3 g and distilled water of 60 ml were required for the preparation of nutrient broth. The above nutrients were added in a beaker according to the quantity specified. Then the distilled water was added and the mixture was checked for pH level of 7 using pH paper. Then the beaker was plugged with cotton and kept inside the pressure cooker for about 15 minutes. Equal quantity of mixture was transferred into the glass plates and kept in the UV chamber for about 10 minutes [20,21].

Treatment of samples with bacterial cultures: The triplicates of SS316L samples A, B, C and D were treated with 5 ml growing culture of *Escherichia coli*, *Bacillus subtilis* and *Klebsiella pneumonia* separately in the sterile disposable petriplates with the finished surface facing the bacterial cultures for the incubation period of 18 hours [22,23]. Then, the samples were then incubated at 37°C for one day. After incubation, the bacterial count on the treated SS316L samples was performed by total plate count method [20,21].

Serial dilution process: Ten test tubes were taken and one among them containing 10 ml of distilled water and other nine test tubes with 9 ml of distilled water. The incubated metal sample was taken and immersed in the test tube containing 10 ml of distilled water and sufficiently stirred. Then 1 ml of this sample was taken and transferred into the test tube containing 9 ml distilled water [20,21]. This process is continued serially for 8 more test tubes and the final sample was taken for the total plate count.

Preparation of nutrient agar: Peptone of 0.25 g, yeast extract of 0.15 g, sodium chloride of 0.25 g, distilled water of 50 ml

and agar of 1.5 g are the required ingredients for the preparation of nutrient agar. The above nutrients were added in a beaker according to the quantity specified and then the distilled water was added. The mixture was checked for pH level of 7 using pH paper. Agar was added and stirred well. Then the beaker was plugged with cotton and kept inside the pressure cooker for about 15 minutes. The mixture was transferred into the glass plate and kept in the UV chamber for about 10 minutes [20,21].

Total plate count method: The prepared nutrient agar was sterilized at 121°C for 15min and then poured into sterile petriplates and allowed for solidification. An aliquot of the serially diluted bacterial culture treated with SS316L samples was added to the solidified agar medium, spread uniformly with a sterile L rod and incubated in an incubator at 37°C for 24 h [20,21]. After incubation, the plates were observed carefully for bacterial colonies and the numbers of colonies were counted for each plate.

Evaluation of inhibitory activity of samples on bacteria: To test the inhibitory potential of SS 316L on *Klebsiella pneumoniae*, the SS316L sample was placed aseptically on petriplates with nutrient agar medium was wiped down with 18 h growing culture. The plates were incubated for 24 hours at 37°C and the region of inhibition was measured if existed [20,21]. Similar procedure was carried out for the other two bacteria also.

Epifluorescence microscopy

For the purpose of fluorescence microscopy, a sample must be fluorescent. Among the various methods of creating a fluorescent sample, the main systematic procedure is labelling by fluorescent stains or, in the case of biological samples, expression of a fluorescent protein. Otherwise, an intrinsic fluorescence of the sample (i.e., auto fluorescence) can be used. In the life sciences, fluorescence microscopy is one of the prevailing tools that allow the specific and sensitive staining of a specimen in order to identify the protein distribution or other molecules of interest. In the present experiment, the acridin orange stainer was used on SS 316L samples containing bacteria is treated for ten minutes [24]. Then the sample was precisely placed in the stage provided in the microscope. Various images of the bacteria containing live and dead cells were taken and saved. These images are used for further analysis.

Results

Surface measurements

The surface roughness parameters of SS316L samples subjected to MRAFF process were measured by CCI along with the 3D surface images (Figure 2). Even though, the average Roughness (Ra) is the most commonly used surface roughness parameter, in order to describe the surface topography in detail, the additional parameters that show the details about the peaks, valleys and their distribution along the

roughness profile were measured and given in Table 3. All these parameters are given in terms of nano meters in the form of mean \pm Standard Deviation (SD).

Table 3. Surface roughness parameters of SS316L samples.

Roughness parameters	Sample A (I=8A)	Sample B (I=6A)	Sample C (I=4A)	Sample D (I=2A)
Average Roughness (Ra) nm	10.52 \pm 0.14	15.78 \pm 0.57	23.4 \pm 0.47	37.4 \pm 0.69
Root mean square deviation of roughness profile (Rq) nm	13.83 \pm 0.52	36.53 \pm 0.63	34.2 \pm 0.89	57.4 \pm 1.12
Maximum height of roughness profile (Rz) nm	36.92 \pm 0.99	80.46 \pm 2.29	208 \pm 2.05	267 \pm 3.36
maximum peak height of roughness profile (Rp) nm	18.58 \pm 0.71	41.86 \pm 1.48	119 \pm 1.42	145 \pm 1.23
Maximum valley depth of roughness profile (Rv) nm	17.83 \pm 0.28	38.06 \pm 0.77	88.5 \pm 0.62	121 \pm 2.1
Total height of roughness profile (Rt) nm	36.41 \pm 0.98	79.92 \pm 2.26	207.5 \pm 2.03	266 \pm 3.32
Skewness (Rsk)	0.087 \pm 0.005	0.91 \pm 0.06	1.44 \pm 0.05	2.22 \pm 0.17
Kurtosis (Rku)	5.36 \pm 0.11	9.31 \pm 0.23	14.6 \pm 0.51	19 \pm 1.32

Table 4. Bacterial adhesions on SS316L samples.

S. No	Sample	<i>Escherichia coli</i>		<i>Klebsiella pneumonia</i>		<i>Bacillus subtilis</i>	
		Initial 10^8	CFU/ml \times Final CFU/ml $\times 10^8$	Initial 10^8	CFU/ml \times Final CFU/ml $\times 10^8$	Initial 10^8	CFU/ml \times Final CFU/ml $\times 10^8$
1	Sample A (R=10.52 nm)		20 \pm 0.82		40 \pm 0.82		38 \pm 0.82
2	Sample B (Ra=15.78 nm)	39 \pm 0.82	22 \pm 1.41	53 \pm 1.41	43 \pm 0.82	51 \pm 0.82	41 \pm 1.41
3	Sample C (Ra=23.4 nm)		24 \pm 0		44 \pm 1.41		43 \pm 0.82
4	Sample D (Ra=37.4 nm)		28 \pm 1.41		47 \pm 0		45 \pm 1.41

Table 5. Bacterial inhibitions on SS316L samples.

S. No	Sample	<i>Escherichia Coli</i>		<i>Klebsiella pneumonia</i>		<i>Bacillus subtilis</i>	
		Initial 10^8	CFU/ml \times Final CFU/ml $\times 10^8$	Initial 10^8	CFU/ml \times Final CFU/ml $\times 10^8$	Initial 10^8	CFU/ml \times Final CFU/ml $\times 10^8$
1	Sample A (R=10.52 nm)		19 \pm 0.82		13 \pm 0.82		13 \pm 0.82
2	Sample B (Ra=15.78 nm)	39 \pm 0.82	17 \pm 1.41	53 \pm 1.41	10 \pm 0.82	51 \pm 0.82	10 \pm 1.41
3	Sample C (Ra=23.4 nm)		15 \pm 0		9 \pm 1.41		8 \pm 0.82
4	Sample D (Ra=37.4 nm)		11 \pm 1.41		6 \pm 0		6 \pm 1.41

Bacterial adhesion-total plate count method result

The results of total plate count are represented in Table 4 in the form of mean \pm SD. The number of Colony Forming Units (CFU)/ml was found to increase with the increase in surface roughness of SS316L samples. The CFU of *E. coli* in sample D was recorded as 28×10^8 and decreased to 20×10^8 in sample A. Similarly, the CFU of *B. subtilis* and *K. Pneumoniae* were recorded as decreased from 45×10^5 to 38×10^8 and 47×10^8 to 40×10^8 in sample D to sample A and sample D to sample

A, respectively. The CFU was calculated by the product of number of colonies and dilution.

The variations of bacterial adhesion as well as inhibition in terms of CFU/ml for each bacteria and SS 316L samples are shown as a bar chart in Figure 3. From the bar chart, it is understood that the increase in surface roughness of SS 316L samples, increases the bacterial adhesion and decreases the inhibition characters (Table 5).

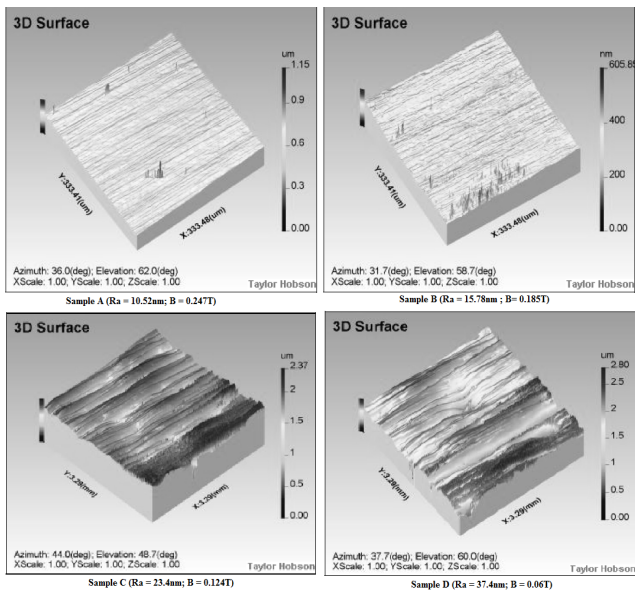


Figure 2. 3D surface images (i) Sample A (ii) Sample B (iii) Sample C (iv) Sample D.

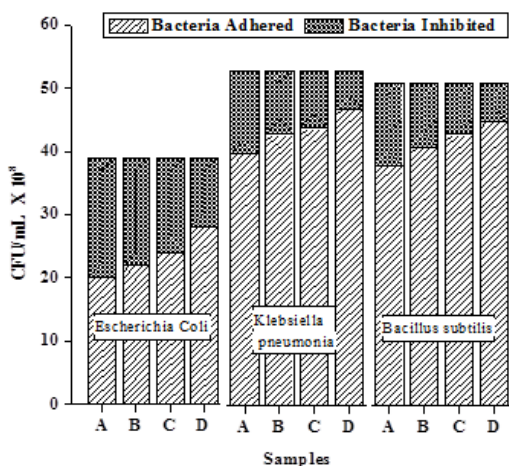


Figure 3. Bacterial adhesion and inhibition of SS 316L samples.

Inhibitory test

A standard inhibitor of chloramphenicol was used to find the difference [25]. In the presence of chloramphenicol, the portion around the standard inhibitor is free from bacterial colonies and the portion around the good surface finish material is surrounded by bacterial colonies of small diameters and around that of the rough surface finish the bacterial colonies of larger diameter were seen as shown in Figure 4. Thus it gives the visual proof that bacterial colonies tend to grow faster in rough surface finish area than that of the fine surface finish area.

Visualization bacterial adhesion

In order to visualize the bacterial adhesion by epifluorescent images, acridin orange was used as the stainer. The bacterial adhesion of *Escherichia coli*, *Klebsiella pneumonia* and *Bacillus subtilis* are shown in Figures 5-7 respectively.

The orange colour in the images represents live cells, green colour represents dead cells and red colour represents the bacteria's excrete. It was also found that acridin orange does not affect the bacteria which are adhered to the metal surface.

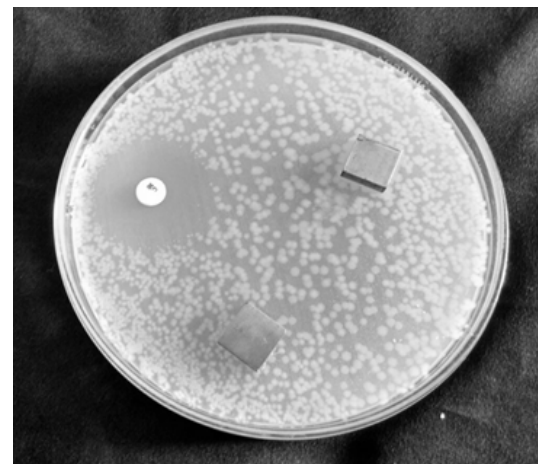


Figure 4. Bacterial inhibition.

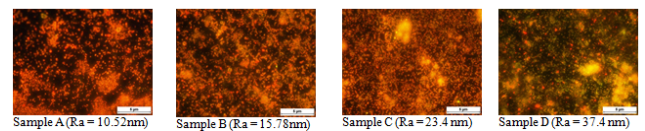


Figure 5. Epifluorescent images of *Escherichia coli* attachment with SS 316L samples.

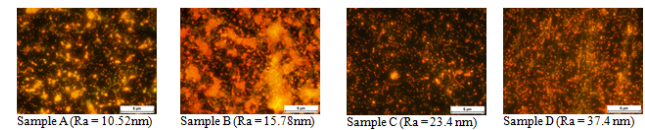


Figure 6. Epifluorescent images of *Klebsiella pneumonia* attachment with SS 316L samples.

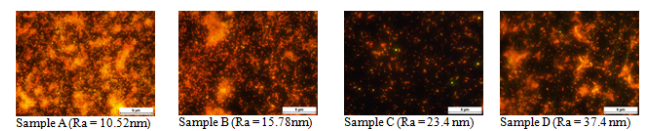


Figure 7. Epifluorescent images of *Bacillus subtilis* attachment with SS 316L samples.

Discussion

In this article, the effects of surface qualities on bacterial adhesion have been studied. Surface finish at nano level was obtained on SS316L samples by means of MRAFF process by varying the magnetic flux density and four different SS316L samples were generated. The surface roughness parameters of the samples were analysed by using talysurf CCI. From the surface measurements of the samples, it is observed that the roughness parameters Ra and Rq were less for the sample A which was subjected to the MRAFF process with highest electromagnetic current (8 A). This is because while the current increases, it leads to the increase in magnetic flux density in turn increases the stiffness of the ferrous particle

chain between the electromagnetic poles and produces higher material removal rate and lower surface roughness values [19]. The highest Ra and Rq were observed in the sample D which was subjected to the MRAFF process with lowest electromagnetic current (2 A). The Rp and Rv are in the increasing order with respect to the decrease in the electromagnetic current. By comparing these Rp and Rv for all the SS316L samples, it is understood that the valley depths are less than the peak heights. In all the samples, Rz is slightly higher than Rt as well as they are in the increasing order with respect to the decrease in the electromagnetic current. All the SS 316L samples exhibited Rsk values greater than zero and Rku greater than 3. It shows that the surfaces are comprised of disproportionate number of peaks as well as sharp peaks along with low valleys [26]. Both Rsk and Rku are in the increasing order with respect to the decrease in the electromagnetic current thus they facilitate the space for bacterial adhesion on the surfaces.

In order to assess the bacterial adhesion, the surface roughness of SS 316L samples were deliberately modified within the nanometer level from 10.52 nm to 37.4 nm by means of MRAFF process. The bacterial adhesion experiments were conducted by means total plate count method and the outcomes of the bacterial culturing demonstrated that surface roughness crucially affects the Colony Forming Units (CFU) of microscopic organisms

Our discoveries are in concurrence with results in the literature. Recently Bohinc [27] and collaborators demonstrated that the rate of adhesion of microscopic organisms on glass surfaces increases with the increase in the surface roughness. Diverse glass surfaces were set up by cleaning the glass plates with various degrees. In such a way the value of roughness was deliberately shifted from a couple of many nanometers to a couple of micrometers. Truong et al. [28] have demonstrated that the bond of bacterial cells *S. aureus* and *P. aeruginosa* on the surfaces of titanium were advanced by the existence of topographical features at nano scale level. Taylor et al. [29] found that a little increment in Ra from 0.04 to 1.24 μm , brought about a huge increment in bacterial bond while a vast increment in Ra from 1.86 to 7.89 μm did not bring about an extremely huge difference in attachment, despite the fact that the grip was still higher than to the smooth surface. Then again Diaz et al. [30,31] have verified that materials with Ra at submicron level, diminish the microbial attachment, while micron level scale advances the microbial bond and Xu et al. [32] have affirmed the results and also clarified the explanations behind it. In the present study, the bacterial adhesion rate on SS 316L surfaces are increasing with the increase in the surface roughness. The increase in surface roughness leads to the increase in the effective surface area and leads to the higher bacterial adhesions. The decrease in the surface roughness restricts the bacterial adhesion as there is less space for accommodating the bacterial colonies, leads to the increase in the bacterial inhibitions.

Conclusion

In the present study, SS 316L sample surfaces were used for bacterial attachment experiments, where the Ra values were at nano level. When the surface roughness of a material is at submicron or nano level, the contact surface available for the bacterial attachment will become less; thereby the tendency of bacterial attachment has come down. We have concentrated only on the effect of surface roughness on bacterial attachment. The hydrophobicity of bacterial cells was not concentrated thus it provides a territory for future examination.

(i) When the SS 316L surface roughness was minimum at the nano meter level, then the adherence of bacteria was less, thus reducing the harmful complications and the method of MRAFF Process proves to be a useful way of surface finishing to the nano level.

(ii) Among the three bacterial cultures selected, the highest bacterial adhesion of 47×10^8 CFU/ml was obtained for *Klebsiella pneumonia* and least bacterial adhesion of 28×10^8 CFU/ml was obtained for *Escherichia coli* for the samples with roughness of 37.4 nm.

(iii) The bacterial inhibition was highest for *Escherichia coli* with 19×10^8 CFU/ml and least for *Klebsiella pneumonia* and *Bacillus subtilis* with 13×10^8 CFU/ml.

(iv) The epifluorescence images ascertain that the bacterial adhesions as well as inhibition on the test samples were influenced by the surface roughness of the samples.

Thus the bacterial attachments were in increasing order when the surface roughness increases but at the same time the bacterial inhibitions were in decreasing order. Therefore nano level smooth surfaces recommended for the implants to resist the bacterial adhesion.

Acknowledgment

The authors acknowledge the ARMATS biotech pvt. Ltd, Chennai for providing technical support for carrying out bacterial culture tests.

References

1. Hermawan H, Ramdan D. Djuansjah JRP. Metals for Biomedical applications. Intech Middle East 2011; 411-430.
2. Riedewald F. Bacterial adhesion to surfaces: the influence of surface roughness. PDA J Pharm Sci Technol 2006; 60: 164-171.
3. Gristina AG, Costerton JW. Bacterial adherence to biomaterials and tissue. The significance of its role in clinical sepsis. J Bone Joint Surg Am 1985; 67: 264-273.
4. An YH, Dickinson RB, Doyle RJ. Mechanism of bacterial adhesion and pathogenic of implant and tissue infections. Totowa Humana Press 2000; 1-27.
5. Dunne WM. Bacterial adhesion: seen any good biofilms lately? Clin Microbiol Rev 2002; 15: 155-166.

6. Palmer J, Flint S, Brooks J. Bacterial cell attachment, the beginning of a biofilm. *J Ind Microbiol Biotechnol* 2007; 34: 577-588.
7. Costerton JW, Stewart PS, Greenberg EP. Bacterial biofilms: a common cause of persistent infections. *Science* 1999; 284: 1318-1322.
8. Advincula MA, Petersen D, Rahemtulla F. Surface analysis and bio corrosion properties of nano structured surface sol-gel coatings on Ti6Al4v titanium alloy implants. *J Biomed Mater Res B Appl Biomater* 2007; 80: 107-120.
9. Bos R, van der Mei HC, Busscher HJ. Physico-chemistry of initial microbial adhesive interactions-its mechanisms and methods for study. *FEMS Microbiol Rev* 1999; 23: 179-230.
10. Quere D, Lafuma A, Bico J. Slippery and sticky micro textured solids. *Nanotechnology* 2003; 14: 1109-1112.
11. Riedewald F. Bacterial adhesion to surfaces: the influence of surface roughness. *PDA J Pharm Sci Technol* 2006; 60: 164-171.
12. Bruinsma GM, Rustema-Abbing M, van der Mei HC, Busscher HJ. Effects of cell surface damage on surface properties and adhesion of *Pseudomonas aeruginosa*. *J Microbiol Methods* 2001; 45: 95-101.
13. Dong H, Onstotta TC, Kob C-HA, Hollingsworth AD, Brown DG, Mailloux BJ. Theoretical prediction of collision efficiency between adhesion-deficient bacteria and sediment grain surface. *Colloid Surf Bio Interf* 2002; 24: 229-245.
14. Mandlik A, Swierczynski A, Das A, Ton-That H. Pili in Gram-positive bacteria: assembly, involvement in colonization and biofilm development. *Trends Microbiol* 2008; 16: 33-40.
15. OToole GA, Kolter R. Flagellar and twitching motility are necessary for *Pseudomonas aeruginosa* biofilm development. *Mol Microbiol* 1998; 30: 295-304.
16. Shellenberger K, Logan BE. Effect of molecular scale roughness of glass beads on colloidal and bacterial deposition. *Environ Sci Technol* 2002; 36: 184-189.
17. Teixeira P, Lopes A, Azeredo J, Oliveira R, Vieira MJ. Physico-chemical surface characterization of a bacterial population isolated from a milking machine. *Food Microbiol* 2005; 22: 247-251.
18. Dunne WM. Bacterial adhesion: seen any good biofilms lately? *Clin Microbiol Rev* 2002; 15: 155-166.
19. Sunil J, Jain VK. Design and development of the magnetorheological abrasive flow finishing (MRAFF) process. *Int J Mach Tool Manufact* 2004; 44: 1019-1029.
20. Holt JG, King NR, Sneath PHA, Staley JT, Williams ST. *Bergeys manual of determinative bacteriology*. Lippincott Williams Wilkins Philadelphia (9th edn.) 2000.
21. Cappuccino JG, Sherman N. *Microbiology- A laboratory manual*. McGraw Hill New York (7th edn.) 2004.
22. An YH, Friedman RJ. Laboratory methods for studies of bacterial adhesion. *J Microbiol Methods* 1997; 30: 141-152.
23. Bjerkan G, Witso E, Bergh K. Sonication is superior to scraping for retrieval of bacteria in biofilm on titanium and steel surfaces in vitro. *Acta Orthop* 2009; 80: 245-250.
24. Gobi K, Vinita V, Ananthakumar R, Ramachandran D, Arul MR. Corrosion, haemocompatibility and bacterial adhesion behaviour of TiZrN-coated 316L SS for bioimplants. *Bull Mater Sci* 2015; 38: 951-955.
25. Wong KY, Vikram P, Kishore KC, Mohammed A. Phytochemical screening and antimicrobial potentials of *Borreria* sps (Rubiaceae). *J King Saud Univ Sci* 2014; 27: 302-311.
26. Gadelmawla ES, Koura MM, Maksoud TMA, Elewa IM, Soliman HH. Roughness parameters. *J Mater Proc Technol* 2002; 123: 133-145.
27. Bohinc K, Drazic G, Fink R, Oder M, Jevsnik M, Nipic D, Torkar KG, Raspor P. Available surface dictates microbial adhesion capacity. *Int J Adhes Adhes* 2014; 50: 265-272.
28. Truong VK, Lapovok R, Estrin YS, Rundell S, Wang JY. The influence of nano-scale surface roughness on bacterial adhesion to ultrafine-grained titanium. *Biomaterials* 2010; 31: 3674-3683.
29. Taylor RL, Verran J, Lees GC, Ward AJ. The influence of substratum topography on bacterial adhesion to polymethyl methacrylate. *J Mater Sci Mater Med* 1998; 9: 17-22.
30. Díaz C, Schilardi PL, Salvarezza RC, de Mele MF. Nano/microscale order affects the early stages of biofilm formation on metal surfaces. *Langmuir* 2007; 23: 11206-11210.
31. Díaz C, Schilardi PL, dos Santos Claro PC, Salvarezza RC, Fernández Lorenzo de Mele MA. Submicron trenches reduce the *Pseudomonas fluorescens* colonization rate on solid surfaces. *ACS Appl Mater Interfaces* 2009; 1: 136-143.
32. Xu LC, Siedlecki CA. Submicron-textured biomaterial surface reduces staphylococcal bacterial adhesion and biofilm formation. *Acta Biomater* 2012; 8: 72-81.

***Correspondence to**

Kathiresan S

Department of Mechanical Engineering

MNM Jain Engineering College

Chennai

India